

Experimental Investigation of Fluid-Structure-Acoustic Interaction in a Rectangular Duct Impedance Facility

*Original*

Experimental Investigation of Fluid-Structure-Acoustic Interaction in a Rectangular Duct Impedance Facility / Fabbri, D., Bruzzone, F., Rosso, C., Avallone, F., Cordioli, J.A., Bonomo, L.A., Pereira, L.M.. - (2026). (32nd AIAA/CEAS Aeroacoustics Conference (2026) Brussels (BEL) 26-29 May 2026) [10.2514/6.2026-3567].

*Availability:*

This version is available at: 11583/3011203 since: 2026-06-15T09:59:57Z

*Publisher:*

American Institute of Aeronautics and Astronautics

*Published*

DOI:10.2514/6.2026-3567

*Terms of use:*

This article is made available under terms and conditions as specified in the corresponding bibliographic description in the repository

*Publisher copyright*

AIAA preprint/submitted version e/o postprint/Author's Accepted Manuscript

(Article begins on next page)

# Experimental Investigation of Fluid-Structure-Acoustic Interaction in a Rectangular Duct Impedance Facility

Daniele Fabbri<sup>\*</sup>, Fabio Bruzzone<sup>†</sup>, Carlo Rosso<sup>‡</sup>, and Francesco Avallone<sup>§</sup>  
*Politecnico di Torino, 10129, Turin, Italy*

Lucas A. Bonomo<sup>¶</sup>, Lucas M. Pereira<sup>||</sup>, and Julio A. Cordioli<sup>\*\*</sup>  
*Federal University of Santa Catarina, 88040-900, Florianópolis, Brazil*

**Fluid-Structure-Acoustic Interaction (FSAI) arises when aerodynamic loading, structural vibration and acoustic propagation are mutually coupled, such that the response of each field influences the others. In ducted systems with flexible walls, this coupling can strongly affect sound transmission and offers potential for passive noise control through controlled structural compliance. This paper reports an experimental investigation of FSAI in a rectangular duct equipped with flush-mounted plates made of three different materials: aluminium, copper, and ABS plastic. The plates were manufactured with identical geometry and tested under the same mounting conditions. A structural characterization was first performed through modal testing. The structure was then subjected to a plane-wave acoustic excitation consisting of discrete pure tones with an amplitude of 130 dB SPL over the frequency range 500-1700 Hz, under no-flow conditions and for centerline Mach numbers of  $M = 0.1$  and  $M = 0.295$ . The transmission loss (TL) was measured for all materials and Mach number combinations. Results show that TL peaks are governed by structural resonances whose mode shapes couple efficiently with the duct acoustic field and are further modified by the mean flow. Copper, despite having modes within the excitation band, yields a flat, near-zero TL, while aluminium produces peaks of up to 9 dB. The presence of a turbulent subsonic flow modifies the plate response, leading in some cases to a shift and amplification of existing resonance peaks, and in others to their suppression. The aim is to provide a benchmark dataset for the future development and validation of multiphysics numerical models, while demonstrating a possible pathway toward noise reduction through controlled structural compliance.**

## I. Introduction

The rapid growth of computational resources and the simultaneous demand for quieter, lighter, and more efficient engineering systems have together elevated Fluid–Structure–Acoustic Interaction (FSAI) to one of the most active research fronts in applied mechanics and acoustics. FSAI concerns the dynamic coupling among aerodynamic flows, structural deformations, and acoustic radiation, which govern noise generation and propagation in a broad spectrum of applications: aircraft fuselage panels, automotive body panels and mirrors, HVAC ducts, renewable energy devices, and biomedical systems such as the human vocal tract [1, 2]. In all these contexts the three physical domains are not independent: flow loads deform the structure, structural motion alters the flow field and radiates sound, and the resulting acoustic field feeds back onto both the structure and the fluid. Capturing this mutual interaction with fidelity requires a unified multiphysics framework, yet the community has historically addressed the constituent couplings between Fluid–Structure Interaction (FSI) and Acoustic–Structure interaction (ASI, or vibroacoustics) as separate problems. The theoretical basis for aeroacoustic sound prediction was established by Lighthill [3], Curle [4] and the most general form was reached by Ffowcs Williams and Hawkings[5], who incorporated arbitrarily moving surfaces through monopole and dipole contributions, enabling the modelling of sound generated by moving bodies and compliant walls. While these formulations provide a general framework for sound generation, early analytical studies of fluid–structure interaction

---

<sup>\*</sup>PhD Student, Department of Mechanical and Aerospace Engineering, Politecnico di Torino, AIAA Student Member.

<sup>†</sup>Assistant Professor, Department of Mechanical and Aerospace Engineering, Politecnico di Torino.

<sup>‡</sup>Associate Professor, Department of Mechanical and Aerospace Engineering, Politecnico di Torino.

<sup>§</sup>Full Professor, Department of Mechanical and Aerospace Engineering, Politecnico di Torino, AIAA Member.

<sup>¶</sup>Postdoctoral Researcher, Laboratory of Vibrations and Acoustics, AIAA Member.

<sup>||</sup>PhD Student, Laboratory of Vibrations and Acoustics, AIAA Student Member.

<sup>\*\*</sup>Associate Professor, Department of Mechanical Engineering, AIAA Member.

revealed additional mechanisms specific to coupled systems. Crighton [6] introduced the concept of neutral wave modes, non-decaying oscillations in coupled fluid–structure systems with mean flow, demonstrating that compliant surfaces can scatter flow energy into acoustic waves even in the absence of classical acoustic sources. Hessesenthaler et al. [7] addressed a critical gap in the FSI modelling community by deriving sixteen fully analytic solutions for FSI problems covering linear and hyperelastic solids, shear driven flows, and quasi-static and transient conditions. These solutions serve as rigorous benchmarks for verifying numerical schemes and assessing spatio-temporal convergence. The extension of FSI numerics to include an explicit acoustic domain, giving the full FSAI problem, is a more recent development driven by applications where acoustic feedback onto the structure or the flow field is significant. One of the first numerical studies to address all three domains simultaneously in a partitioned framework was the work of Schäfer et al. [8]. Their configuration, a thin flexible plate in the wake of a bluff body inside a duct, used LES with the parallel multigrid solver [9] for the fluid, a finite element method for the structure and acoustics [10], and the MpCCI interface [11] for time-step-based data exchange. The weak vibroacoustic coupling relied on Lighthill’s analogy [3] with no acoustic feedback onto the flow or structure. Comparison with wind-tunnel experiments [12] confirmed that the approach reproduced dominant tonal peaks, though peak amplitudes were overestimated due to the absence of structural damping. Springer et al. [13] conducted a thorough experimental investigation of a flat plate excited by a turbulent backward facing step flow, comparing one sided coupling, aerodynamic loads drive the structure without acoustic feedback, with two sided coupling in which the acoustic pressure acts on the structure simultaneously. Their results [14] showed that acoustic feedback introduces significant radiation damping, reducing structural vibration amplitudes and the radiated sound pressure level at resonant frequencies, demonstrating that one sided coupling systematically overestimates structural response at eigenfrequencies. Kolb and Schäfer [15] proposed a coupled aeroacoustic framework for flexible structures in low-Mach-number turbulent flows combining LES with an ALE formulation for mesh motion, an acoustic/viscous splitting method [16, 17] for the acoustic field, and a partitioned coupling implemented through the preCICE library [18]. Validation against membrane airfoil experiments [19, 20] demonstrated that structural flexibility significantly alters the aeroacoustic field and that membrane oscillations enhance low-frequency sound radiation through vortex-structure interaction. Huang [21, 22] provided one of the main reference frameworks for the study of acoustic and structural interaction in ducts. Through analytical modelling and experiments on flexible panels, an impedance matrix formulation was developed to describe the coupled response of the duct system to incident acoustic waves and the associated structural motion. The experimental confirmation of the predicted fluid loading regimes [23] established a benchmark that has subsequently guided both numerical validation campaigns and the development of compliant acoustic liner concepts. Building on this analytical framework, Fan et al. [24] developed a fully coupled numerical time domain approach based on the space time Conservation Element and Solution Element method, CE/SE [25]. This formulation enabled the simultaneous resolution of the compressible flow, acoustic field and structural dynamics without introducing a separate acoustic domain. Their simulations, performed for Mach numbers between 0.1 and 0.5, revealed bimodal flexural wave propagation along the membrane, with two distinct waves travelling in opposite directions. Since this behaviour could not be explained only by convective Doppler shifting, it highlighted the complex interaction between acoustic compressibility, mean flow and structural compliance. Following the same general direction, d’Elia [26] investigated a compact passive liner concept based on cantilevered vibrating beams coupled with backing cavities and resistive micro slits. In this configuration, the flexible element was not a continuous flush-mounted plate, but an array of articulated beam like resonators designed to enhance low frequency acoustic absorption. The liner was characterized under normal and grazing acoustic incidence, also in the presence of grazing flow, and a simplified impedance model was proposed to predict its attenuation performance. More recently, Lam [27] investigated a configuration more closely related to the present study by testing membrane type acoustic metamaterial liners under grazing mean flow and extracting reflection, absorption and transmission loss. In this context, grazing mean flow refers to the steady flow imposed along the duct, parallel to the compliant surface, and is quantified here by the corresponding Mach number. Lam [27] reported measurements up to approximately  $M=0.12$ , providing relevant evidence of the acoustic behaviour of compliant liners under low grazing flow conditions. These works are particularly useful for visualizing the behaviour of a structure exposed simultaneously to grazing flow and acoustic excitation, a configuration that shares several features with acoustic liner methodologies [28–31]. However, in these recent experimental studies the analysis was mainly based on global acoustic quantities, whereas the structural response of the compliant surface was not directly measured. This limits the possibility of identifying the coupling mechanisms between the acoustic field, the grazing flow and the flexible structure. These studies therefore highlight the need for controlled benchmark datasets in enclosed ducts, where acoustic coefficients and full field structural vibration data are acquired simultaneously, or under matched operating conditions, for different flexible materials and grazing flow regimes. The present study addresses this gap with two complementary objectives. The first objective is to generate

an experimental dataset suitable for the validation and calibration of multiphysics numerical models of flow, acoustic and structural coupling in ducts. The second objective is to assess whether controlled structural flexibility can be exploited as a passive mechanism for reducing acoustic transmission under grazing flow conditions. To this end, three flush-mounted plates with the same geometry and mounting conditions, but with different material properties, are tested. In this sense, the work is designed as a parametric experimental study in which the plate material is varied while the geometry and boundary conditions are kept fixed. This approach allows the influence of structural characteristics, such as stiffness, density and damping, on the interaction with both the acoustic field and the turbulent grazing flow to be assessed. In addition, the experiments extend the range of grazing flow conditions considered in the previous works discussed above, since the present study also includes higher Mach number conditions. The experimental workflow is designed to separate and then correlate the main physical contributions involved in the coupled response. First, each plate is structurally characterized in order to identify its modal properties. The plates are then installed in the duct and tested under harmonic acoustic excitation at different grazing flow Mach numbers. For each flow condition, the plate velocity is also measured without acoustic excitation, so that the vibration induced by the grazing flow alone can be distinguished from the acoustically forced response. The response under tonal acoustic excitation is finally compared across materials and Mach numbers by combining transmission loss, reflection and absorption coefficients with full field structural vibration measurements. This combined analysis makes it possible to assess how the mechanical properties of the structure and the flow speed influence the coupling between the acoustic field, the grazing flow and the flexible plates. Beyond the specific experimental results, the resulting dataset is intended to support numerical validation and calibration, while also providing physical insight into the potential of flexible structures as low noise duct treatments based on controlled structural flexibility.

## II. Experimental Setup

### A. Plate and support details

Three rectangular panels with identical dimensions were tested, with length  $L = 420$  mm, height  $H = 100$  mm, and thickness  $T = 1$  mm were manufactured from aluminium (AL1), copper (COP1), and ABS plastic (PLA1). Figure 1 shows the aluminium plate mounted in the sample holder (SH) which is the central part of the impedance tube test rig, presented in the next sections. The plates present two flaps located along the short edges specifically introduced to ensure proper clamping of the panel and to achieve a fully clamped mounting. The structure is flush-mounted; embedding

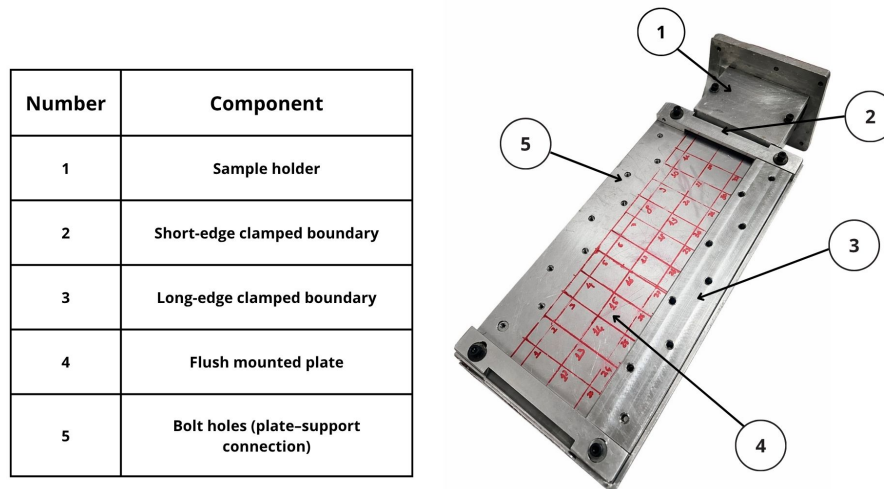


**Fig. 1 Plate mounted in the sample holder**

the structure perfectly within the sample holder is intended to avoid introducing geometric discontinuities that could generate additional vorticity in the flow. In this work, the flexible plate is not treated as a passive boundary, but rather as an active dynamic component whose flexibility and material properties play a fundamental role in governing the coupling mechanisms. By systematically varying the elastic modulus, density, and damping characteristics, it is possible

to control the flexibility of the structure and, consequently, its interaction with the surrounding flow and acoustic fields. Table 1 summarizes the three classes of materials used for the plates. By varying the ratio between  $m'$  (defined as the product of thickness  $h$  and mass density  $\rho$ ) and the bending stiffness  $D$ , different values of the bending wavenumber  $k_b$  and the coincidence frequency  $f_c$  can be obtained. The interplay between these parameters governs the degree of coupling between structural motion and the acoustic field, thereby affecting both energy transmission and attenuation mechanisms. In the case of acoustic excitation, the coincidence frequency identifies the condition at which the phase velocity of the bending wave matches that of the acoustic wave. Around this frequency, the coupling between the structure and the acoustic field becomes particularly strong, leading to highly efficient radiation and sound transmission through the plate. Below this condition, the structure behaves as a poor radiator because of the mismatch between the bending and acoustic wavenumbers. In contrast, for turbulent boundary layer (TBL) excitation [32], the energy transfer depends on the matching between the convective wavenumber  $k_c = \frac{\omega}{U_c}$  (with  $U_c$  the convective velocity) of the turbulent pressure fluctuations and the structural bending wavenumber  $k_b$ . When  $k_b$  approaches  $k_c$ , convective coincidence occurs, allowing efficient coupling between the flow and the structure. This mechanism dominates the flow-induced vibration regime. Moreover based on the works of [33, 34] the mechanical impedance of the three materials has been calculated using the simplified model of an infinite plate.

**Table 1** Nominal mechanical properties of the tested panels and corresponding dynamic parameters for a 1 mm thick plate.

Material	$E$ [GPa]	$\rho$ [ $\text{kg m}^{-3}$ ]	$\nu$	$k_b$ [ $\text{m}^{-1}$ ] (1 kHz)	$f_c$ [Hz]	$D/m'$	$Z_\infty$ [ $\text{N s m}^{-1}$ ]
Aluminum (AL1)	70	2700	0.33	63.5	12025	2.43	303
Copper (COP1)	110	8960	0.34	76.4	17409	1.16	694
ABS plastic (PLA1)	3.5	1250	0.36	110.2	36164	0.268	47

## B. Test rig description

The FSAI experiment is carried out in the Federal University of Santa Catarina (UFSC) Grazing Flow Acoustic Impedance Facility, the duct has a rectangular cross section with width  $W = 40$  mm and height  $H = 100$  mm. A three-dimensional schematic of the rig is presented in Figure 2. Quasi-anechoic terminations are installed at both the inlet and outlet to minimize acoustic reflections, while compression drivers located upstream and downstream of the test section generate controlled acoustic fields of 150 dB can be generated in both directions, i.e. in both upstream and downstream directions relative to the mean flow. The grazing flow is provided by an external compressed air supply, allowing Mach numbers up to  $M = 0.7$ . The flow velocity is controlled using a differential pressure transmitter connected to a 2 mm diameter Pitot tube mounted at the duct inlet and calibrated according to ISO 3966:2008 [35]; the flow temperature is monitored continuously by a dedicated temperature sensor.

## C. Test matrix and data post-processing

The test matrix was designed to evaluate the coupled acoustic and structural response of the panels under controlled combinations of acoustic excitation and grazing flow: the incoming plane wave was provided by the compression drivers at an incident sound pressure level of approximately 130 dB selected to maximize the signal-to-noise ratio while avoiding non linear effects. Eight flush-mounted microphones, four upstream and four downstream of the test section, were used to reconstruct the incident, reflected, and transmitted wave components through a mode-matching approach [36, 37]. Panel vibration was measured using a scanning Laser Doppler Vibrometer (LDV), while modal testing was performed to independently identify the structural properties of the mounted plate. The experimental campaign considered tonal excitation at 25 discrete frequencies between 500 Hz and 1700 Hz, together with broadband excitation over the same frequency range. Tests were performed without flow and under centerline grazing flow conditions at  $M = 0.100$  and  $M = 0.295$ . For each condition, surface velocity, microphone signals and flow control parameters were acquired. Microphone data were post processed using a Welch based spectral estimation procedure, with the compression drivers signal used as reference. This allowed the reflection, transmission and absorption coefficients to be evaluated. Data were acquired at a sampling frequency of 12.8 kHz, using 30 averages of 12800 samples with 75% overlap. Further details on the methodology are reported in [29]. The same procedure was repeated for all tested materials in order to assess the influence of structural properties on the coupled vibroacoustic response.

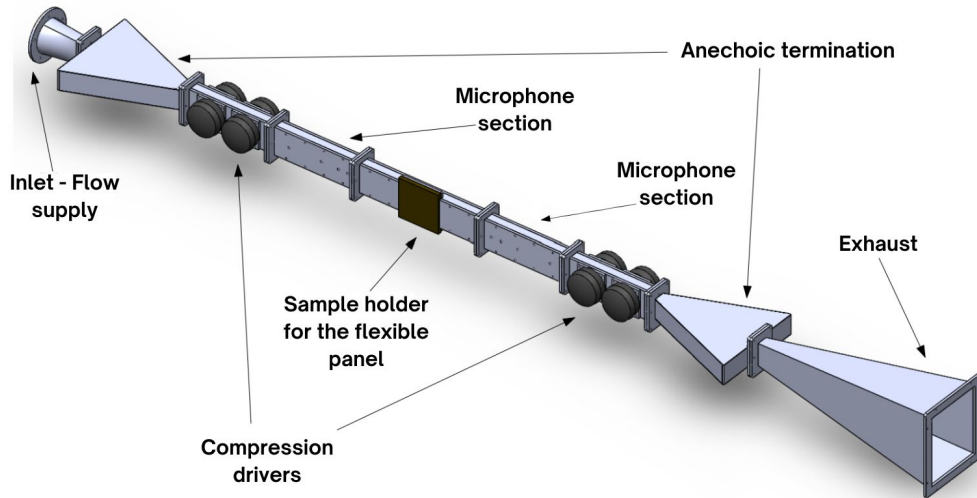


Fig. 2 UFSC Impedance Tube Test Rig.

### III. Results

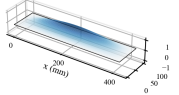
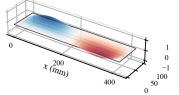
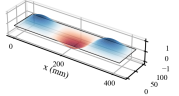
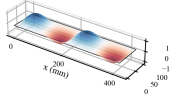
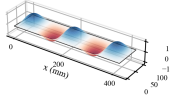
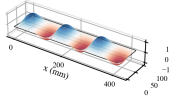
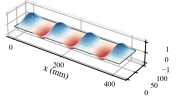
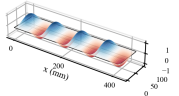
#### A. Structural modal parameters

The three material plates were characterized by experimental modal analysis. Each specimen was mounted in the same sample holder and under the same mounting conditions used for the impedance duct tests, while the complete sample holder assembly was suspended in a free free condition. Excitation was provided by a shaker, and the structural response was measured using a scanning LDV. A set of 33 measurement points was distributed over the plate surface. Their positions were selected using the MoGeSeC algorithm [38] in order to optimize the spatial sampling for modal identification. A broadband excitation signal from 10 Hz to 3.2 kHz, with a total duration of 30 s, was applied to excite the structural modes within the frequency range of interest. The experimental setup is shown in Figure 3. Table 2 reports the first eight experimentally identified modes, including the corresponding eigenfrequencies, damping ratios and mode shapes. Modal parameters were extracted from the frequency domain data using standard modal curve fitting techniques. The results indicate that the mounted plate behaves approximately as a fully clamped structure. Indeed, the identified mode shapes, also reported in Table 2, are consistent with those expected for a rectangular plate with four clamped edges, namely a C-C-C-C boundary condition, as described in [39].

#### B. Structural and acoustic results

In this section, both the acoustic and structural performance of the tested flexible structures are presented. The acoustic field is analysed in terms of transmission loss, absorption coefficient and reflection coefficient, together with the structural response measured by the laser vibrometer. The acoustic quantities were computed from the incident, reflected and transmitted wave amplitudes reconstructed from the eight flush-mounted microphone signals using the mode matching procedure detailed in [36, 37]. In particular, the transmission and reflection coefficients were obtained as the ratios between the transmitted and incident wave amplitudes, and between the reflected and incident wave amplitudes, respectively. The absorption coefficient was then evaluated from the corresponding acoustic energy balance. Transmission loss quantifies the reduction between the incoming wave upstream and the transmitted wave downstream of the plate, while the absorption and reflection coefficients describe the portions of acoustic energy that are dissipated and reflected by the presence of the structure. At the same time, the vibrometer measurements allow the structural dynamics to be directly related to the observed acoustic behaviour. Figure 4 shows the structural response of the plates

**Table 2 Identified modal parameters with simply-supported plate mode shapes (first 8 modes).**

Mode	Shape ( $m, n$ )	Aluminum (AL1)		Copper (COP1)		Plastic (PLA1)	
		$f_d$ (Hz)	Damp (%)	$f_d$ (Hz)	Damp (%)	$f_d$ (Hz)	Damp (%)
	Mode (1,1)						
1		535.20	0.768	413.69	0.325	151.13	0.494
	Mode (2,1)						
2		591.04	1.305	489.17	0.436	227.98	0.244
	Mode (3,1)						
3		637.83	0.484	523.22	0.174	265.44	0.316
	Mode (4,1)						
4		685.57	0.420	592.16	0.634	385.75	0.237
	Mode (5,1)						
5		739.31	0.853	686.53	0.110	457.05	0.247
	Mode (6,1)						
6		816.28	0.169	801.08	0.777	541.73	0.135
	Mode (7,1)						
7		973.45	0.872	906.38	0.511	588.14	0.161
	Mode (8,1)						
8		1093.88	0.193	1097.09	0.642	667.21	0.058



**Fig. 3** Modal analysis test rig.

under flow excitation only. The reported spectra were obtained by averaging the velocity power spectral density (PSD) over all measurement points acquired with the scanning laser vibrometer. The results highlight a strong dependence of the vibration response on both material properties and Mach number. As expected, increasing the Mach number produces a general increase in vibration level for all tested materials. However, this effect is particularly pronounced for the plastic plate, which exhibits the highest response over most of the investigated frequency range. This behaviour can be attributed to its lower mechanical impedance, which makes the structure more sensitive to the unsteady pressure fluctuations generated by the grazing flow. At  $M = 0.295$ , the separation between the plastic response and those of the metallic plates becomes especially evident in the mid frequency range. The aluminium plate exhibits a response mainly governed by its first structural modes, indicating that the flow excitation effectively couples with the lower order modal behaviour of the panel. In contrast, the plastic plate does not show a response clearly associated with its first modes, but rather exhibits a broader vibration pattern extending towards higher frequencies, suggesting the activation of higher order structural contributions. The copper plate generally shows the lowest vibration levels, consistent with its higher mechanical impedance, mainly resulting from its high material density. All three materials exhibit a peak around 150 Hz, which is associated with a characteristic of the flow inside the duct rather than with the structural dynamics of the plates. The same peak is also observed in the microphone spectra of a fully rigid configuration, which is not reported here for the sake of brevity. The same behaviour is highlighted in Figure 5, where the average PSD reports the average value as a function of the Mach number, comparing the response of the two materials, highlighting also the eigenfrequencies found above indicated by vertical dotted lines. For aluminium and copper, shown in panels **a** and **b**, respectively, a shift of the resonant peaks is observed. This phenomenon can be attributed to the well-known fluid mass-spring effect, whereby the surrounding moving fluid modifies the effective dynamic properties of the coupled system, leading to resonance frequencies different from those identified in the in vacuo modal analysis. This effect is widely reported in the literature on fluid structure interaction [40, 41]. In contrast, the plastic plate, shown in panel **c**, does not exhibit the same clear frequency shift trend. Instead, its response again indicates a stronger tendency to vibrate through higher order modes rather than being dominated by the first structural resonances. This suggests that, for the most flexible material, the flow-induced excitation is distributed over a broader modal range, leading to a more complex structural response. Overall, these results indicate that, in the absence of acoustic forcing, the plate response is governed primarily by the interaction between the turbulent wall pressure field and the structural mobility of each material [32, 42]. The comparison therefore provides a baseline for interpreting the acoustically forced cases, where the measured vibration will result from the superposition of flow induced excitation and acoustic loading. Figure 6 reports the case with grazing turbulent flow and acoustic excitation. For clarity, the response measured without acoustic excitation is also included over the same frequency range, in order to provide a baseline for comparison. The three

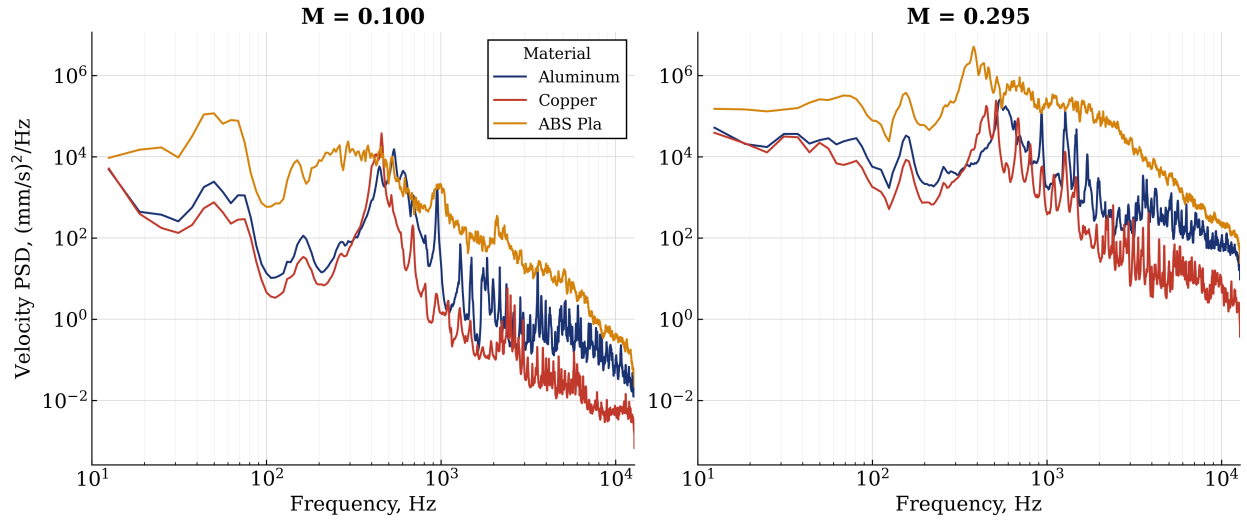


**Fig. 4** Average surface vibration velocity PSD of the plate under only flow excitation - Material comparison

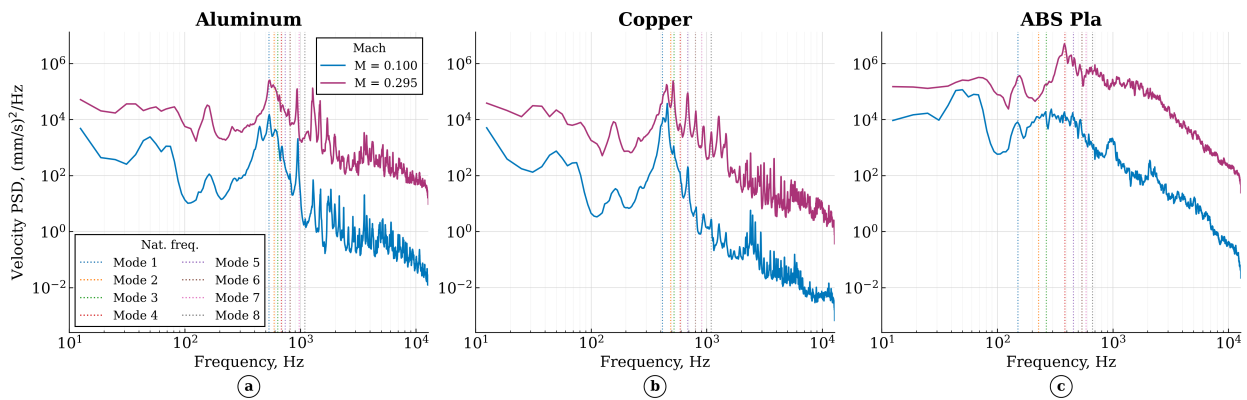


**Fig. 5** Average surface vibration velocity PSD of the plate under only flow excitation - Mach number

materials exhibit markedly different behaviours. For the aluminium plate, shown in panel **a**, the presence of grazing turbulent flow only slightly modifies the structural response, producing a small shift in the natural frequencies. It is also evident that the seventh mode, located slightly below 1000 Hz, couples efficiently with the acoustic excitation in both configurations. For the copper plate, shown in Figure **6b**, the first structural mode is clearly visible below 500 Hz. As the Mach number increases, this peak appears to shift towards lower frequencies. Since the acoustic excitation is applied as a set of discrete tones in the frequency range between 500 Hz and 1700 Hz, with a frequency step of 50 Hz, this first mode lies outside the excited frequency band. Therefore, although the copper plate may potentially contribute to the acoustic response through this low-frequency mode, this contribution is not captured in the present acoustic results because the mode is not directly excited. Therefore, the incoming acoustic wave at 130 dB does not excite the first modal peaks, and the resulting vibration levels remain lower than those observed for aluminium. Finally, consistently with the modal data reported in Table 2, the plastic plate is mainly excited through higher order modes. Its response is concentrated in the frequency range between 950 Hz and 1100 Hz, with amplitudes comparable to those measured for the aluminium plate. The acoustic results provide insight into the influence of structural dynamics on the overall

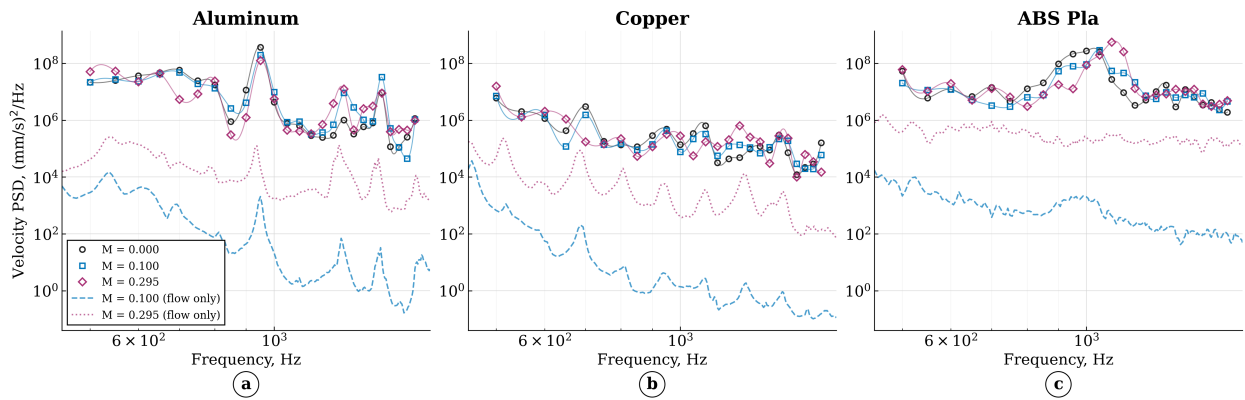


**Fig. 6 Average surface vibration velocity PSD of the plate under acoustic and flow excitation - Mach number**

transmission behaviour of the test rig. As shown in Figure 7, the highest transmission loss is obtained for the aluminium plate, reported in panel **a**. However, its behaviour changes when acoustic excitation is combined with grazing flow. Under the zero mean flow condition, the transmission loss exhibits a broader response, particularly in the low frequency range, whereas in the presence of flow the response becomes narrower and more localized. This behaviour may be related to a modification of the structural response induced by the mean flow, together with a different coupling between the acoustic field radiated by the vibrating structure and the incoming plane wave. In the low frequency range, the transmission loss of the aluminium plate is mainly governed by reflection of the incident acoustic wave, as indicated by the reflection and absorption coefficients reported in Figures 8 and 9. Values of the reflection coefficient higher than unity may be associated with spurious reflections from the quasi anechoic terminations of the test rig or, less likely, with residual uncertainties in the wave decomposition procedure, which was nevertheless validated against independent measurements. The zero Mach number case also shows additional contributions at higher frequencies, around 950 Hz and 1100 Hz. According to the absorption coefficient, these peaks suggest that part of the acoustic energy is dissipated through an absorption mechanism associated with the vibrating structure. It is important to note, however, that higher transmission loss is not directly correlated with larger vibration amplitudes. As shown in Figure 6, the strongest structural response occurs around 950 Hz, but this peak does not always correspond to an increase in transmission loss. In particular, the contribution of the higher order modes to transmission loss appears slightly more pronounced at  $M = 0.1$  than at  $M = 0$ . However, when the Mach number is further increased, the same frequency range no longer provides a clear contribution to transmission loss, even though significant structural vibration is still observed. This indicates that the structural response alone is not sufficient to explain the acoustic performance of the plate. Rather, the effectiveness of these modes depends on their coupling with the acoustic field inside the duct, which is modified by the grazing mean flow. As expected, the plastic case, reported in panel **c**, exhibits the most complex behaviour among the three materials. In this case, the combination of acoustic excitation and the highest Mach number produces the largest relative transmission loss values, although with a significant frequency shift. This behaviour can be related to the lower mechanical impedance of the plastic plate compared with the other materials, which makes it more sensitive to the unsteady pressure fluctuations generated by the grazing turbulent flow. The absorption coefficient

further suggests that, for the plastic plate, a relevant portion of the incident acoustic energy is dissipated through the compliant flush-mounted structure. Therefore, the observed transmission loss appears to be mainly associated with a structural absorption mechanism, rather than with a predominantly reflective acoustic response. The opposite trend is observed for the copper plate, reported in panel **b**: owing to its high density and mechanical impedance, copper exhibits a much weaker vibration response over the analysed frequency range, resulting in limited coupling with the acoustic field and a comparatively small contribution to transmission loss.

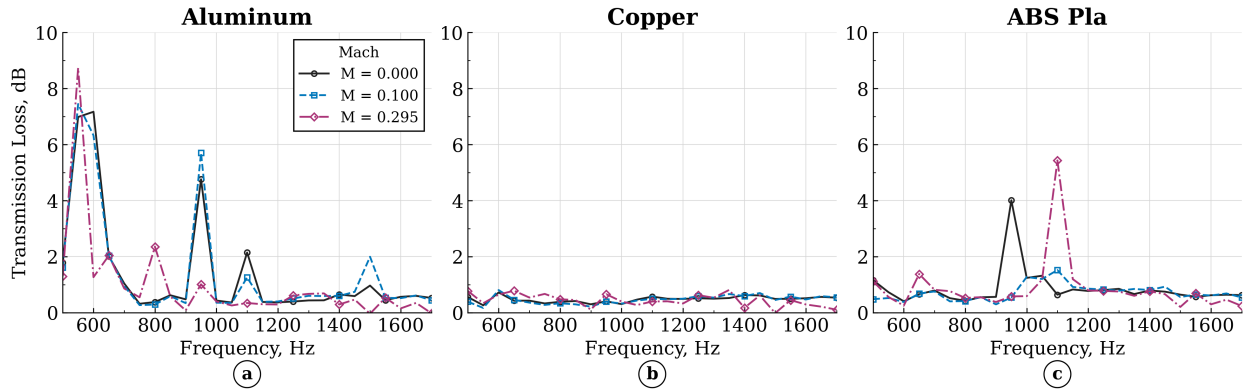


**Fig. 7** Transmission loss of the three materials for different Mach numbers.

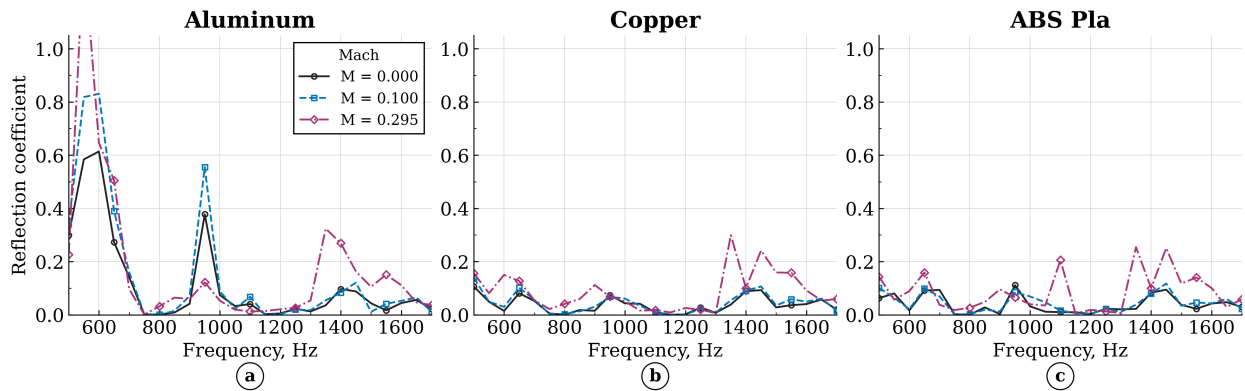


**Fig. 8** Reflection coefficient of the three materials for different Mach numbers.

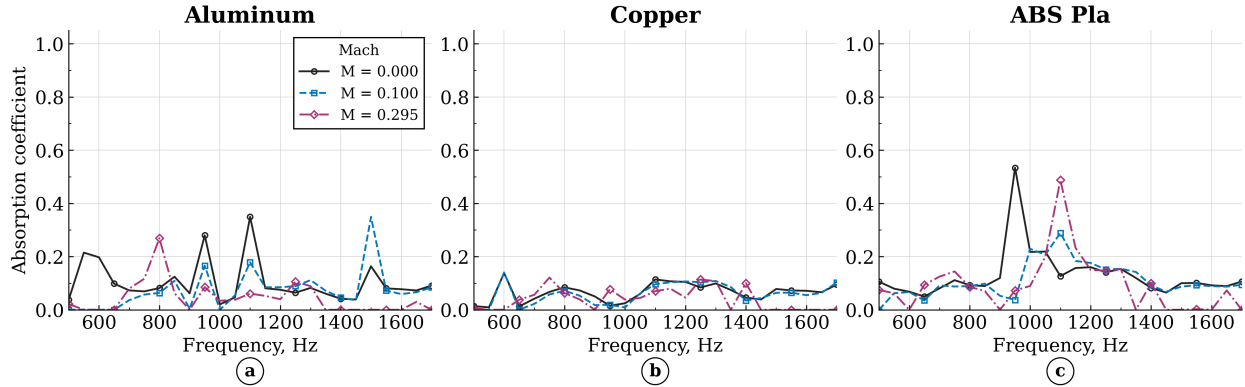


**Fig. 9 Absorption coefficient of the three materials for different Mach numbers.**

#### IV. Conclusions

This work investigated the acoustic field inside a grazing flow impedance tube with the presence of flexible panels. The aim of the work was to characterise the coupled structural and acoustic response as a function of material properties and Mach number. Three materials were considered, namely aluminium, copper and ABS plastic, covering a broad range of stiffness, mass per unit area and damping characteristics. Acoustic performance was assessed in terms of transmission loss, reflection and absorption coefficients, while the structural response was measured using a scanning laser vibrometer, allowing panel dynamics to be correlated with the acoustic behaviour. The results show that transmission loss arises from the interaction between structural response, acoustic field and the hydrodynamic forcing induced by the turbulent flow. Aluminium provided the highest transmission loss, mainly associated with reflection of the incident acoustic wave in the low frequency range, instead, for the ABS panel, a twofold effect was observed. First, the influence of grazing flow became more pronounced as the Mach number increased, producing a frequency shift of the system response towards higher frequencies. Second, this shift was accompanied by a stronger contribution of the absorption coefficient. Therefore, the absorption mechanisms associated with the ABS panel are not fixed in frequency, but vary with Mach number together with the coupled structural and acoustic response. The copper plate, owing to its high mechanical impedance, contributed only weakly to acoustic attenuation because of its limited structural response. Overall, these findings confirm that changing structural impedance can significantly influence acoustic transmission in ducted systems and may therefore be exploited in the design of noise reduction configurations. Future work should focus on clarifying how the presence of the flexible structure modifies the acoustic field inside the duct. In particular, further analyses are needed to distinguish between energy dissipation mechanisms associated with structural motion and mechanisms related to the generation of an additional reflected acoustic field, which may contribute to reducing the incident wave level. In addition, the large amplitude vibrations observed for the most flexible panel suggest that structural motion may also feedback on the grazing flow, potentially promoting energy dissipation directly within the flow field rather than only through the generation of a reflected acoustic field. In addition, the experimental campaign provided a comprehensive dataset in which the effects of the incident acoustic field, grazing flow and structural motion of the flexible plates can be analysed within the same framework. This makes the dataset a relevant basis for the validation and calibration of numerical models aimed at reproducing fluid-structure-acoustic interaction in ducted systems.

#### V. Acknowledgments

This publication is part of the project PNRR-NGEU which has received funding from the MUR – DM 117/2023.

#### References

- [1] Schoder, S., Falk, S., Wurzinger, A., Lodermeier, A., Becker, S., and Kniesburges, S., “A Benchmark Case for Aeroacoustic Simulations Involving Fluid-Structure-Acoustic Interaction Transferred from the Process of Human Phonation,” *Acta Acustica*, Vol. 8, 2024. <https://doi.org/10.1051/aacus/2024005>.
- [2] Maurerlehner, P., Schoder, S., Freidhager, C., Wurzinger, A., Hauser, A., Kraxberger, F., Falk, S., Kniesburges, S., Echternach, M., Döllinger, M., and Kaltenbacher, M., “Efficient numerical simulation of the human voice: simVoice – a three-dimensional

- simulation model based on a hybrid aeroacoustic approach,” *e i Elektrotechnik und Informationstechnik*, 2021. <https://doi.org/10.1007/s00502-021-00886-1>.
- [3] Lighthill, M. J., “On Sound Generated Aerodynamically. I. General Theory,” *Proceedings of the Royal Society of London. Series A. Mathematical and Physical Sciences*, Vol. 211, No. 1107, 1952, pp. 564–587. <https://doi.org/10.1098/rspa.1952.0060>.
- [4] Curle, N., “The Influence of Solid Boundaries upon Aerodynamic Sound,” *Proceedings of the Royal Society of London Series A*, Vol. 231, No. 1187, 1955, pp. 505–514. <https://doi.org/10.1098/rspa.1955.0191>.
- [5] Williams, J. E. F., and Hawkings, D. L., “Sound Generation by Turbulence and Surfaces in Arbitrary Motion,” *Philosophical Transactions of the Royal Society of London Series A*, Vol. 264, No. 1151, 1969, pp. 321–342. <https://doi.org/10.1098/rsta.1969.0031>.
- [6] Crighton, D. G., and Oswell, J. E., “Fluid Loading with Mean Flow. I. Response of an Elastic Plate to Localized Excitation,” *Philosophical Transactions of the Royal Society of London Series A*, Vol. 335, No. 1639, 1991, pp. 557–592. <https://doi.org/10.1098/rsta.1991.0060>.
- [7] Hessesenthaler, A., Balmus, M., Röhrle, O., and Nordsletten, D., “A Class of Analytic Solutions for Verification and Convergence Analysis of Linear and Nonlinear Fluid-Structure Interaction Algorithms,” *Computer Methods in Applied Mechanics and Engineering*, Vol. 362, 2020, p. 112841. <https://doi.org/10.1016/j.cma.2020.112841>.
- [8] Schafer, F., Muller, S., Uffinger, T., Becker, S., Grabinger, J., and Kaltenbacher, M., “Fluid-Structure-Acoustic Interaction of the Flow Past a Thin Flexible Structure,” *AIAA Journal*, Vol. 48, No. 4, 2010, pp. 738–748. <https://doi.org/10.2514/1.40344>.
- [9] Durst, F., and Schäfer, M., “A Parallel Blockstructured Multigrid Method for the Prediction of Incompressible Flows,” *International Journal for Numerical Methods in Fluids*, Vol. 22, 1996, pp. 549–565.
- [10] Schoder, S., and Roppert, K., “openCFS: Open Source Finite Element Software for Coupled Field Simulation – Part Acoustics,” Tech. rep., ??? Working paper.
- [11] Schäfer, F., Kniesburges, S., Uffinger, T., Becker, S., Grabinger, J., Link, G., and Kaltenbacher, M., “Numerical Simulation of Fluid-Structure- and Fluid-Structure-Acoustic Interaction Based on a Partitioned Coupling Scheme,” *High Performance Computing in Science and Engineering, Garching/Munich 2007*, edited by S. Wagner, M. Steinmetz, A. Bode, and M. Brehm, Springer Berlin Heidelberg, Berlin, Heidelberg, 2009, pp. 335–348.
- [12] Becker, S., Lienhart, H., and Durst, F., “Flow Around Three-Dimensional Obstacles in Boundary Layers,” *Journal of Wind Engineering and Industrial Aerodynamics*, Vol. 90, No. 4, 2002, pp. 265–279. [https://doi.org/10.1016/S0167-6105\(01\)00209-4](https://doi.org/10.1016/S0167-6105(01)00209-4).
- [13] Springer, M., Scheit, C., and Becker, S., “Fluid-Structure-Acoustic Coupling for a Flat Plate,” *International Journal of Heat and Fluid Flow*, Vol. 66, 2017, pp. 249–257. <https://doi.org/10.1016/j.ijheatfluidflow.2017.04.013>.
- [14] Blake, W. K., *Mechanics of Flow-Induced Sound and Vibration, Volume 2: Complex Flow-Structure Interactions*, Academic Press, 2017.
- [15] Kolb, E., and Schäfer, M., “Aeroacoustic Simulation of Flexible Structures in Low Mach Number Turbulent Flows,” *Computers & Fluids*, Vol. 227, 2021, p. 105020. <https://doi.org/10.1016/j.compfluid.2021.105020>.
- [16] Guasch, O., Pont, A., Baiges, J., and Codina, R., “Finite Element Hybrid and Direct Computational Aeroacoustics at Low Mach Numbers in Slow Time-Dependent Domains,” *Computers & Fluids*, Vol. 239, 2022, p. 105394. <https://doi.org/10.1016/j.compfluid.2022.105394>.
- [17] Hardin, J. C., and Pope, D. S., “An Acoustic/Viscous Splitting Technique for Computational Aeroacoustics,” *Theoretical and Computational Fluid Dynamics*, Vol. 6, No. 5, 1994, pp. 323–340. <https://doi.org/10.1007/BF00311844>.
- [18] Uekermann, B., Bungartz, H.-J., Yau, L., Chourdakis, G., and Rusch, A., “Official preCICE Adapters for Standard Open-Source Solvers,” , 2017.
- [19] Rojratsirikul, P., Wang, Z., and Gursul, I., “Unsteady Fluid–Structure Interactions of Membrane Airfoils at Low Reynolds Numbers,” *Experiments in Fluids*, Vol. 46, 2010, pp. 859–872. <https://doi.org/10.1007/s00348-009-0623-8>.
- [20] Rojratsirikul, P., Wang, Z., and Gursul, I., “Effect of Pre-Strain and Excess Length on Unsteady Fluid–Structure Interactions of Membrane Airfoils,” *Journal of Fluids and Structures*, Vol. 26, No. 3, 2010, pp. 359–376. <https://doi.org/10.1016/j.jfluidstructs.2010.01.005>.

- [21] Huang, L., “A Theoretical Study of Duct Noise Control by Flexible Panels,” *The Journal of the Acoustical Society of America*, Vol. 106, No. 4, 1999, pp. 1801–1809. <https://doi.org/10.1121/1.427930>.
- [22] Huang, L., “A Theoretical Study of Passive Control of Duct Noise Using Panels of Varying Compliance,” *The Journal of the Acoustical Society of America*, Vol. 109, No. 6, 2001, pp. 2805–2814. <https://doi.org/10.1121/1.1369108>.
- [23] Huang, L., Choy, Y. S., So, R. M., and Chong, T. L., “Experimental Study of Sound Propagation in a Flexible Duct,” *The Journal of the Acoustical Society of America*, Vol. 108, No. 2, 2000, pp. 624–631. <https://doi.org/10.1121/1.429594>.
- [24] Fan, K. H., et al., “Computational Aeroacoustic-Structural Interaction in Internal Flow with CE/SE Method,” , 2018.
- [25] Lam, G., Leung, R., Yu, K. F., and Tang, S. K., “Computational Duct Aeroacoustics Using CE/SE Method,” 2008. <https://doi.org/10.2514/6.2008-2824>.
- [26] d’Elia, M. E., “Flow-Acoustic Interaction with Innovative Materials,” Ph.D. thesis, Le Mans Université, December 2021. URL <https://theses.hal.science/tel-03588310>.
- [27] Lam, K. H., “Experimental and Numerical Studies of Low-Frequency Duct Acoustic Liner Using Metamaterial Technology,” Ph.D. thesis, The Hong Kong Polytechnic University, Hong Kong, 2022.
- [28] Tam, C., Kurbatskii, K., Ahuja, K., and Gaeta, R., “A Numerical and Experimental Investigation of the Dissipation Mechanisms of Resonant Acoustic Liners,” *Journal of Sound and Vibration*, Vol. 245, No. 3, 2001, pp. 545–557. <https://doi.org/10.1006/jsvi.2001.3571>.
- [29] Spillere, A., Bonomo, L., Cordioli, J., and Brambley, E., “Experimentally Testing Impedance Boundary Conditions for Acoustic Liners with Flow: Beyond Upstream and Downstream,” *Journal of Sound and Vibration*, 2020, p. 115676. <https://doi.org/10.1016/j.jsv.2020.115676>.
- [30] Avallone, F., and Damiano, C., *Acoustic-induced velocity in a multi-orifice acoustic liner grazed by a turbulent boundary layer*, ????. <https://doi.org/10.2514/6.2021-2169>, URL <https://arc.aiaa.org/doi/abs/10.2514/6.2021-2169>.
- [31] Avallone, F., Bosia, F., Chen, Y., Colombo, G., Craster, R., Ponti, J. M. D., Fabbiane, N., Haberman, M. R., Hwang, W., Iemma, U., Juhl, A., Kadic, M., Kotsonis, M., Laude, V., Marquet, O., Mery, F., Michelis, T., Nouh, M., Ragni, D., Touboul, M., Wegener, M., and Krushynska, A. O., “Metamaterials and Fluid Flows,” , 2025. ArXiv:2509.05371.
- [32] Corcos, G., “The resolution of turbulent pressures at the wall of a boundary layer,” *Journal of Sound and Vibration*, Vol. 6, No. 1, 1967, pp. 59–70. [https://doi.org/https://doi.org/10.1016/0022-460X\(67\)90158-7](https://doi.org/https://doi.org/10.1016/0022-460X(67)90158-7), URL <https://www.sciencedirect.com/science/article/pii/0022460X67901587>.
- [33] Buhler, K., “Driving point impedances of thick homogeneous plates in flexure,” *Journal of Sound and Vibration*, Vol. 78, No. 2, 1981, pp. 235–245. [https://doi.org/https://doi.org/10.1016/S0022-460X\(81\)80035-1](https://doi.org/https://doi.org/10.1016/S0022-460X(81)80035-1), URL <https://www.sciencedirect.com/science/article/pii/S0022460X81800351>.
- [34] Cremer, L., Heckl, M., and Petersson, B. A. T., *Structure-Borne Sound: Structural Vibrations and Sound Radiation at Audio Frequencies*, 3<sup>rd</sup> ed., Springer Berlin, Heidelberg, 2005. <https://doi.org/10.1007/b137728>.
- [35] “Measurement of fluid flow in closed conduits – Velocity area method using Pitot static tubes,” , 2008. Standard.
- [36] Bonomo, L. A., Quintino, N. T., Cordioli, J. A., Avallone, F., Jones, M. G., Howerton, B. M., and Nark, D. M., *A Comparison of Impedance Education Test Rigs with Different Flow Profiles*, ????. <https://doi.org/10.2514/6.2023-3346>, URL <https://arc.aiaa.org/doi/abs/10.2514/6.2023-3346>.
- [37] Quintino, N. T., Bonomo, L. A., Pereira, L. M., Cordioli, J. A., and Avallone, F., *Boundary Layer Effects on Experimental Impedance Education*, ????. <https://doi.org/10.2514/6.2024-3022>, URL <https://arc.aiaa.org/doi/abs/10.2514/6.2024-3022>.
- [38] Bonisoli, E., Delprete, C., and Rosso, C., “Proposal of a modal-geometrical-based master nodes selection criterion in modal analysis,” *Mechanical Systems and Signal Processing*, Vol. 23, No. 3, 2009, pp. 606–620. <https://doi.org/https://doi.org/10.1016/j.ymsp.2008.05.012>, URL <https://www.sciencedirect.com/science/article/pii/S0888327008001386>.
- [39] Leissa, A., *Vibration of Plates*, NASA SP, Scientific and Technical Information Division, National Aeronautics and Space Administration, 1969. URL <https://books.google.it/books?id=TfsfAAAAIAAJ>.
- [40] Abdullah, A., Leung, R. C., Lam, R. K., Naseer, M. R., and Arif, I., “Mitigation of Broadband Duct Flow Noise Using Liner with Gradient Surface Resonant Compliance,” *Journal of Fluids and Structures*, Vol. 140, 2026, p. 104452. <https://doi.org/10.1016/j.jfluidstructs.2025.104452>.

- [41] Fahy, F., and Gardonio, P., *Sound and Structural Vibration: Radiation, Transmission and Response*, Academic Press, Elsevier/Academic, 2007.
- [42] Hambric, S., Hwang, Y., and Bonness, W., “Vibrations of plates with clamped and free edges excited by low-speed turbulent boundary layer flow,” *Journal of Fluids and Structures*, Vol. 19, No. 1, 2004, pp. 93–110. <https://doi.org/10.1016/j.jfluidstructs.2003.09.002>, funding Information: The authors acknowledge gratefully financial support from the Office of Naval Research (ONR) Code 334, Stephen Schreppler, contract monitor. Copyright: Copyright 2017 Elsevier B.V., All rights reserved.